

Original Research

Preclinical studies for improving radiosensitivity of non-small cell lung cancer cell lines by combining glutaminase inhibition and senolysis

Masaki Fujimoto, Ritsuko Higashiyama, Hironobu Yasui, Koya Yamashita, Osamu Inanami*

Laboratory of Radiation Biology, Department of Applied Veterinary Sciences, Faculty of Veterinary Medicine, Hokkaido University, Sapporo 060-0818, Japan



ARTICLE INFO

Keywords:

Radiation
Glutaminolysis
Senescence
Senolytic drug
Apoptosis

ABSTRACT

Glutamine metabolism, known as glutaminolysis, is abnormally activated in many cancer cells with *KRAS* or *BRAF* mutations or active c-MYC. Glutaminolysis plays an important role in the proliferation of cancer cells with oncogenic mutations. In this study, we characterized radiation-induced cell death, which was enhanced by glutaminolysis inhibition in non-small cell lung cancer A549 and H460 cell lines with *KRAS* mutation. A clonogenic survival assay revealed that treatment with a glutaminase inhibitor, CB839, enhanced radiosensitivity. X-irradiation increased glutamate production, mitochondrial oxygen consumption, and ATP production, whereas CB839 treatment suppressed these effects. The data suggest that the enhancement of glutaminolysis-dependent energy metabolism for ATP production is important for survival after X-irradiation. Evaluation of the cell death phenotype revealed that glutaminolysis inhibitory treatment with CB839 or a low-glutamine medium significantly promoted the proliferation of β -galactosidase-positive and IL-6/IL-8 secretory cells among X-irradiated tumor cells, corresponding to an increase in the senescent cell population. Furthermore, treatment with ABT263, a Bcl-2 family inhibitor, transformed senescent cells into apoptotic cells. The findings suggest that combination treatment with a glutaminolysis inhibitor and a senolytic drug is useful for efficient radiotherapy.

Introduction

Many cancers with mutations (such as *KRAS* [1,2] or *BRAF* [3] mutations) or c-MYC activation [4] and triple-negative breast cancers [5] are reported to be dependent on glutamine as a source of nutrition for cell proliferation and homeostasis maintenance. The upregulation of glutaminolysis in these cancers is attributed to an increase in the expression of glutaminase (GLS) and the glutamine transporter (SLC1A5) [6–9]. Glutaminolysis upregulation in cancer cells is considered to be important for maintaining the mitochondrial tricarboxylic acid cycle for energy production through the electron transport chain (ETC) in tumors with oncogene mutations [10].

Cancer-specific glutaminolysis-related metabolism has attracted attention as a target for cancer therapy. Reportedly, the chemical or genomic inhibition of GLS and SLC1A5 suppresses cell proliferation and

induces death in lung cancer [8], pancreatic cancer [11], melanoma [9], and triple-negative breast cancer cells [5]. The inhibition of glutamine metabolism has also been reported to enhance the tumor-cell-killing efficiency of radiotherapy or chemotherapy. For example, bis-2-(5-phenylacetamido-1,2,4-thiadiazol-2-yl) ethyl sulfide, a GLS1 inhibitor, enhanced not only the radiation-induced loss of clonogenic activity in non-small cell lung cancer cells [11], but also cisplatin and paclitaxel sensitivity in ovarian cancer cells [12]. Moreover, compound 968, a GLS inhibitor, was shown to sensitize ovarian cancer cells to paclitaxel [13], and glutamine deprivation was shown to increase cisplatin- or etoposide-induced neuroblastoma cell death [14]. Yang et al. demonstrated that, as novel effects of glutaminolysis inhibition, GLS inhibition (via the glutamine antagonist 6-diazo-5-oxo-L-norleucine), short hairpin RNA interference against GLS, and glutamine depletion in the medium strongly induced senescence in

Abbreviations: ETC, electron transport chain; GLS, glutaminase; SLC1A5, glutamine transporter; SA- β -gal, senescence-associated beta galactosidase; SASP, senescence-associated secretory phenotype; CDK, cyclin-dependent kinase; MAPK, mitogen-activated protein kinase; MPM, malignant pleural mesothelioma; EMT, epithelial-to-mesenchymal transition; DMEM, Dulbecco's modified Eagle's medium; FBS, fetal bovine serum; HRP, horseradish peroxidase; PBS, phosphate-buffered saline; OCR, oxygen consumption rate; ESR, electron spin resonance; BSA, bovine serum albumin; PI, propidium iodide; ELISA, enzyme-linked immunosorbent assay; SDS-PAGE, sodium dodecyl sulfate-polyacrylamide gel electrophoresis; TBST, Tris-buffered saline-Tween 20.

* Corresponding author.

E-mail addresses: masaki_fujimoto@vetemed.hokudai.ac.jp (M. Fujimoto), ritsu3322@gmail.com (R. Higashiyama), yassan@vetemed.hokudai.ac.jp (H. Yasui), koyamashita@vetemed.hokudai.ac.jp (K. Yamashita), inanami@vetemed.hokudai.ac.jp (O. Inanami).

<https://doi.org/10.1016/j.tranon.2022.101431>

Received 8 October 2021; Received in revised form 18 March 2022; Accepted 11 April 2022

1936-5233/© 2022 The Authors. Published by Elsevier Inc. This is an open access article under the CC BY-NC-ND license (<http://creativecommons.org/licenses/by-nc-nd/4.0/>).

pancreatic cancer 8988 T cells [15]. Although the induction of senescence in cancer cells is reportedly related to mitochondrial energy metabolism in osteosarcoma cells [16], fibroblast cells [17], and endothelial cells [18,19], it remains unclear whether cellular senescence plays a major role in radiosensitization and chemosensitization induced by the sublethal inhibition of glutaminolysis in tumor cells.

Physiologically, senescence refers to the stable arrest of the cell cycle, which is caused by the shortening of telomeres as the cell divides and reaches the limit of division (Hayflick limit) [20]. Conversely, immortalized cells and cancer cells also undergo senescence, known as premature senescence, which is caused by oncogene mutations [21] and exogenous DNA damage [22]. Senescent cells are characterized by changes in the expression patterns of several biomarkers, such as the activation of senescence-associated beta galactosidase (SA- β -gal), overexpression of p53, p21 CIP1 (p21), and p16INK4A (p16), and secretion of a large number of factors, including growth factors, cytokines, chemokines, and proteases, which collectively constitute the senescence-associated secretory phenotype (SASP) [23,24]. Among the cellular mechanisms underlying the induction of senescence, severe oxidative stress, gamma and UVB irradiation, and treatment with several anticancer drugs activate p53 to induce the overexpression of the cyclin-dependent kinase (CDK) inhibitor, p21, and stimulate p16, which is followed by the induction of senescence [23,24]. As a different senescence pathway from the p53/p21 axis or the p16 pathway, the DNA damage-induced activation of MKK3/6 and p38 δ mitogen-activated protein kinase (MAPK) plays an important role in the induction of the p53-independent pathway in oncogene (RAS/RAF)-induced senescence [25,26].

Although cellular senescence is irreversible arrest of cell proliferation, an increase in cellular senescence is not considered to be beneficial in cancer therapy [27,28], because it leads to the secondary secretion of various SASP-related factors, such as inflammatory cytokines, IL-1, IL-6, IL-8 (which cause chronic inflammation), TGF- β (which stimulates proliferation by promoting angiogenesis), and proteases (which promote carcinogenesis) [29]. For example, in malignant pleural mesothelioma (MPM) cells, treatment with conditioned medium containing SASP-related factors reportedly induced epithelial-to-mesenchymal transition (EMT) and led the cells to acquire chemoresistance against the anticancer folic acid metabolic antagonist pemetrexed [30]. Therefore, two strategies have been proposed for cancer therapy to prevent SASP-induced side effects: inhibition of the secretion of SASP factors [31,32] and conversion of senescence to apoptosis by senolytic agents [33–35]. Reportedly, the suppression of IL-6 and IL-1 α secretion from radiation-induced senescent fibroblast cells by the mTOR inhibitor rapamycin inhibits the migration or growth of prostate cancer cells [31]. The senolytic drug ABT263, which is an inhibitor of the Bcl-2 family of anti-apoptotic proteins, including Bcl-2, Bcl-W, and Bcl-X_L, has also been reported to induce the transition of therapy-induced senescence to apoptosis in breast cancer cells and lung cancer cells [33].

In the present study, we demonstrated the enhancement of radiosensitivity in response to glutaminolysis inhibition in human lung adenocarcinoma cells and evaluated the attributed cell death phenotype. The increase in the senescent cell population contributed significantly to the radiation-sensitizing effect. In addition, we investigated the effect of the senolytic drug ABT263 on the induction of senescence and showed that ABT263 induced the transition from senescence to apoptosis, the latter being the preferred mode of cell death in therapy.

Materials and methods

Cell culture

Human lung cancer cell lines, A549 and H460, were obtained from the Riken Cell Bank and the American Type Culture Collection, respectively. A549 cells were cultured in Dulbecco's modified Eagle's medium (DMEM; Sigma-Aldrich, St. Louis, MO, USA) supplemented with 25 mM

glucose, 4 mM glutamine, 1 mM sodium pyruvate, and 10% (v/v) fetal bovine serum (FBS; Biosera, Nuaille, France). H460 cells were incubated in RPMI1640 medium (Thermo Fisher Scientific, MA, USA) supplemented with 10% (v/v) FBS. The cell cultures were maintained at 37 °C in 5% CO₂.

Reagents and antibodies

The GLS inhibitor CB839 was purchased from MedChem Express (South Brunswick, NJ, USA). The Bcl-2/Bcl-X_L inhibitor ABT263 was purchased from Cayman Chemical (Ann Arbor, MI, USA). Glutamine and L-[2,3,4,–³H] were purchased from Moravec Inc. (Brea, CA, USA). Anti-p53, anti-p21, anti-actin, anti-cyclin A, anti-cyclin B1, and horseradish peroxidase (HRP)-conjugated secondary antibodies were obtained from Santa Cruz Biotechnology (Santa Cruz, CA, USA). An anti-p-CDK2 (Thr160) antibody was purchased from Cell Signaling Technology (Danvers, MA, USA).

X-irradiation

X-irradiation was performed using an X-RAD iR-225 (Precision X-Ray, North Branford, CT, USA) with a dose rate of 1.37 Gy/min at 200 kVp, 15 mA, with a 1.0 mm aluminum filter.

Clonogenic survival assay

Cells were seeded in 60 mm ϕ dishes (Thermo Fisher Scientific) and incubated for 6 h. The attached cells were X-irradiated (1, 2, 4, or 8 Gy) and incubated with or without CB839 (4 nM for A549 cells and 40 nM for H460 cells). The cell colonies were fixed with methanol and stained with Giemsa stain. Cells from colonies containing more than 50 cells were scored as surviving cells.

Glutamine uptake and glutamate production

X-irradiation was performed 24 h before measurement, and 10 μ M CB839 was administered 1 h before measurement. Glutamine uptake and glutamate production in the cells were measured according to a partially modified version of a method reported by Mongin et al. [36]. In the experiments regarding glutamine metabolism and oxygen consumption rate (OCR), a relatively high concentration (10 mM) was employed unlike other radiosensitivity experiments, since the objective was only to confirm the inhibitory effect of CB839 on them for a short time under conditions where cell death by CB839 would not cause cell number changes. The cells were seeded in a 35 mm ϕ dish and incubated overnight. DMEM supplemented with 50 nM glutamine, L-[2,3,4,–³H] (6 μ Ci) was added to the cells, and the cells were incubated at 37 °C in 5% CO₂. Following this, the cells were washed with 1 mL of cold phosphate-buffered saline (PBS) three times on ice. The cells were then mixed with 1 mL of cold PBS, removed by a cell scraper, and collected in 1.5 mL tubes. The cells were lysed by sonication, and the obtained cell lysate was applied to an anion exchange resin (AG 1-X8 Polyprop Chromatography Columns, Bio-Rad Laboratories, Hercules, CA, USA) to isolate ³H-labeled glutamate synthesized by cellular GLS from glutamine, L-[2,3,4,–³H]. The resin was washed three times with 2 mL of water, and the washing solution was collected for the measurement of glutamine uptake in the cells through amino acid transporters present in the plasma membrane. The adsorbate in the column was eluted three times with 2 mL of 0.1 N HCl, and the eluent was collected for the measurement of glutamate synthesized by cellular glutamine. One milliliter of washing solution with water or the eluent with 0.1 N HCl solution was mixed with 5 mL of a liquid scintillator (AQUASOL-2; PerkinElmer, Waltham, MA, USA). ³H radioactivity was measured using an LSC-5100 instrument (Hitachi, Tokyo, Japan).

Measuring oxygen consumption rate (OCR) by electron spin resonance (ESR)

OCR was measured using ESR, as previously reported [37–41]. X-irradiation was performed 24 h before measurement, and 10 μM CB839 was administered 1 h before measurement.

ATP measurement

ATP measurement was performed using the “Cell” ATP assay reagent (Toyo B-Net, Tokyo, Japan) according to the manufacturer’s instructions. Cells were collected from 35 mm ϕ dish by trypsinization, and cell suspensions were prepared at 1.0×10^5 cells/mL. One hundred microliters of the cell suspensions were added to 96-well plates, and the ATP assay reagent was added. Cellular ATP levels were measured using a VICTOR Nivo Multimode Microplate Reader (PerkinElmer).

Evaluation of DNA damage

Cells were seeded on a coverslip in a 35 mm ϕ dish and incubated overnight. Ten nM CB839 was administered immediately after X-irradiation, and the cells were incubated for 0.5, 1, 2, 6, or 24 h. Cells were fixed with 4% paraformaldehyde in PBS for 10 min. Cells were permeabilized with PBS containing 0.3% Triton-X, and then washed three times with 1 mL of PBS. Non-specific antibody binding was blocked with PBS containing 6% bovine serum albumin (BSA) for 60 min at room temperature. The blocked cells were incubated overnight with an anti- γH2AX antibody (1:1,000) or anti-53BP1 antibody in PBS containing 1% BSA and 0.3% Triton-X at 4 °C. Next, the cells were incubated for 1.5 h in the dark with an Alexa Fluor® 488 anti-rabbit antibody (1:1,000) in PBS containing 1% BSA and 0.3% Triton-X at room temperature. After incubation, the cells were washed three times with PBS and counterstained with 300 nM DAPI for 5 min at room temperature. The coverslips were mounted with ProLong® Gold Antifade Mountant reagent (Thermo Fisher Scientific). Fluorescence microscopic analysis was performed using an Olympus BX61 microscope (Olympus, Tokyo, Japan). The number of γH2AX foci or 53BP1 foci per cell was counted. At least 100 cells were analyzed.

SA- β -gal assay

To analyze cellular senescence, a senescence-associated β -galactosidase staining kit (Cell Signaling Technology) was used according to the manufacturer’s instructions. Cells were seeded in a 35 mm ϕ dish and incubated overnight. A549 and H460 cells were X-irradiated (5 Gy) and then incubated for 5 and 3 days, respectively. After incubation, the cells were fixed with a fixing solution for 10 min at room temperature. The fixed cells were washed three times with PBS. The cells were treated with 1 mL of an SA- β -gal staining solution and incubated overnight at 37 °C. The solution was replaced with 70% glycerol, and images of the cells were acquired using a BZ-9000 instrument (KEYENCE, Osaka, Japan). At least 200 cells were analyzed. SA- β -gal-positive cells were counted, and the percentage of SA- β -gal-positive cells among total cells was calculated.

Apoptosis analysis by flow cytometry

Cells were seeded in a 60 mm ϕ dish and incubated overnight. A549 and H460 cells were irradiated with 5 Gy X-ray and incubated for 3 and 2 days, respectively. The cells were collected in 15 mL tubes by trypsinization. The cells were centrifuged at 1,000 rpm for 5 min at 4 °C, and the supernatant was removed. The cells were suspended in PBS, and 2.0×10^5 cells were collected in a 1.5 mL tube. The sample was centrifuged at 1,000 rpm for 5 min at 4 °C, and the supernatant was removed. The cells were suspended in 450 μL of binding buffer (10 mM HEPES, 150 mM NaCl, 5 mM KCl, and 2.5 mM CaCl_2). APC annexin-V (Thermo

Fisher Scientific) was added to the tube, and the mixture was incubated for 15 min at room temperature. Following this, the cells were stained with 5 μL of propidium iodide (PI) for 5 min at room temperature, and 1.0×10^5 cells were analyzed for apoptosis using BD FACSVerser™ (Becton, Dickinson and Company, Tokyo, Japan). Annexin-V single-positive cells were considered early apoptotic cells, and annexin-V and PI double-positive cells were considered late apoptotic cells or necrotic cells.

Enzyme-linked immunosorbent assay (ELISA)

The levels of IL-6 and IL-8 in the culture medium were measured using ELISA MAX™ Deluxe set (BioLegend, San Diego, CA, USA) according to the manufacturer’s instructions. Cells were seeded in a 60 mm ϕ dish and incubated overnight. Next, the cells were X-irradiated (5 Gy) and incubated for 5 days. The culture medium was collected in a 15 mL tube. A coating buffer containing a capture antibody (1:200) was added to a 96-well plate, and the plate was incubated overnight at 4 °C. After this, the plate was washed four times with 300 μL of wash buffer (PBS containing 0.05% Tween). To block non-specific binding, 200 μL of the assay diluent was added to the plate, and the plate was incubated at room temperature for 1 h with shaking. After washing the plate with 300 μL of wash buffer four times, 100 μL of each sample was added to each well, and the plate was incubated at room temperature for 2 h with shaking. The plate was washed four times with 300 μL of wash buffer. An assay diluent (100 μL) with detection antibody (1:200) was added to each well, and the plate was incubated at room temperature for 1 h with shaking. The plate was washed four times with 300 μL of wash buffer. Avidin-horse radish peroxidase solution (100 μL) was added to the plate, and the plate was incubated at room temperature for 1 h with shaking. The plate was washed five times with 300 μL of wash buffer. TMB substrate solution (100 μL) was added to the plate, following which the plate was incubated at room temperature for 15 min in the dark. After incubation, a stop solution was added to each well, and the level of IL-6 was determined by measuring the absorbance at 450 nm using a VICTOR Nivo Multimode Microplate Reader (PerkinElmer). The levels of IL-6 or IL-8 were normalized by the cell number at the endpoint.

Western blotting

After the indicated treatment, the cells were collected in a 1.5 mL tube with a scraper. The cells were centrifuged at 10,000 rpm for 1 min at 4 °C, and the supernatant was removed. The cell pellets were added to a lysis buffer (50 mM Tris-HCl [pH 7.5], 1% Triton-X, 5% glycerol, 5 mM EDTA, and 150 mM NaCl) and subjected to freeze-thawing. Following this, the pellets were centrifuged at 15,000 rpm for 15 min at 4 °C, and the supernatant was collected in a new 1.5 mL tube. The protein concentration in the supernatant was measured using a Bio-Rad Protein Assay Kit (Bio-Rad Laboratories) according to the manufacturer’s instructions, and the protein concentration in each sample was standardized. The samples were added to half the volume of sodium dodecyl sulfate-polyacrylamide gel electrophoresis (SDS-PAGE) loading buffer (composed of 0.125 M Tris-HCl (pH 6.8), 10% 2-mercaptoethanol, 4% sodium dodecyl sulfate, 4% glycerol, and 0.004% bromophenol blue) and boiled for 1 min. The samples were separated by SDS-PAGE and transferred to a nitrocellulose membrane (Advantec Toyo, Tokyo, Japan). The membrane was blocked with Tris-buffered saline-Tween 20 (TBST; 10 mM Tris-HCl (pH 7.4) and 0.1% Tween-20) containing 5% skimmed milk for 1 h at room temperature. The membrane was treated overnight with primary antibodies against p53 (1:1,000), p21 (1:1,000), cyclin A (1:1,000), cyclin B (1:1,000), p-CDK2 (Thr160) (1:1,000), and actin (1:2,000) in TBST containing 5% skimmed milk at 4 °C. Next, the membrane was treated with an HRP-conjugated secondary antibody (1:2,000) for 1 h at room temperature. Blots were developed using Western Lightning Plus-ECL (PerkinElmer) and detected using an LAS 4000 mini (Fujifilm, Tokyo, Japan).

Statistical analysis

Results are expressed as the mean \pm SD of values obtained from three experiments. The variance ratio was estimated using the F-test, and two-group comparisons were performed using the Student's *t*-test or Welch's *t*-test. Dunnett's test was performed for multiple comparisons. The minimum level of significance was set at $P < 0.05$.

Results

CB839, a GLS inhibitor, enhanced radiation sensitivity

At first, to evaluate the pharmacological effect of a GLS inhibitor, CB839, we investigated glutamine uptake and glutamate production by using ^3H -labeled glutamine [36]. X-irradiation significantly increased the glutamine uptake, but CB839 did not affect the glutamine uptake in A549 and H460 cells (Figs. S1A and S2A). Glutamate conversion from glutamine was increased by X-irradiation, and this increase was inhibited by CB839 treatment in both cell lines (Figs. S1B and S2B). Next, we performed OCR measurement with ESR in order to contribution of glutaminolysis in TCA cycle and mitochondrial ETC. X-irradiation significantly increased the mitochondrial oxygen consumption, and CB839 inhibited this increase (Fig. S1C). In parallel, the X-irradiation-induced enhancement of ATP production was also inhibited by CB839 (Fig. S1D). Reportedly, a mitochondrial complex I inhibitor

rotenone decreased oxygen consumption rate and cellular ATP level in human promyelocytic leukemia cell line HL-60 cells [42], and treatment of metformin, which have the complex I inhibitory activity, inhibited oxygen consumption and ATP production in canine osteosarcoma cell line HMPOS [43]. We also previously reported the relationship between decreased mitochondrial ATP production caused by inhibition of OCR and radiosensitivity in a study based on the inhibition of the mitochondrial electron transport system by lipophilic triphenylphosphonium derivatives in HeLa cells and A549 cells [39].

To examine the effect of the CB839 on radiation sensitivity in lung cancer cells, a colony formation assay was performed. The sublethal doses of CB839 in a 2-week treatment for A549 and H460 cells were estimated at 4 nM (Fig. S3A) and 40 nM (Fig. S4A), respectively. In addition, 10 nM CB839 had no effect on cell survival for 5 days in A549 cells (Fig. S3B). A549 and H460 cells were treated with sublethal doses of CB839 immediately after X-irradiation. Treatment with a sublethal dose of CB839 after X-irradiation significantly decreased the survival fraction of both cell lines (Figs. 1A and S4B). Since radiation-induced cell death is primarily mediated by DNA damage, immunofluorescence staining for γH2AX and 53BP1, which are DNA damage markers, was performed to investigate whether glutaminolysis inhibition affects DNA damage and the DNA repair capability after X-irradiation. CB839 treatment after X-irradiation did not affect γH2AX (Fig. 1B) and 53BP1 (Fig. 1C) foci formation. These results suggest that the radiation-induced activation of glutaminolysis-dependent ATP production through the

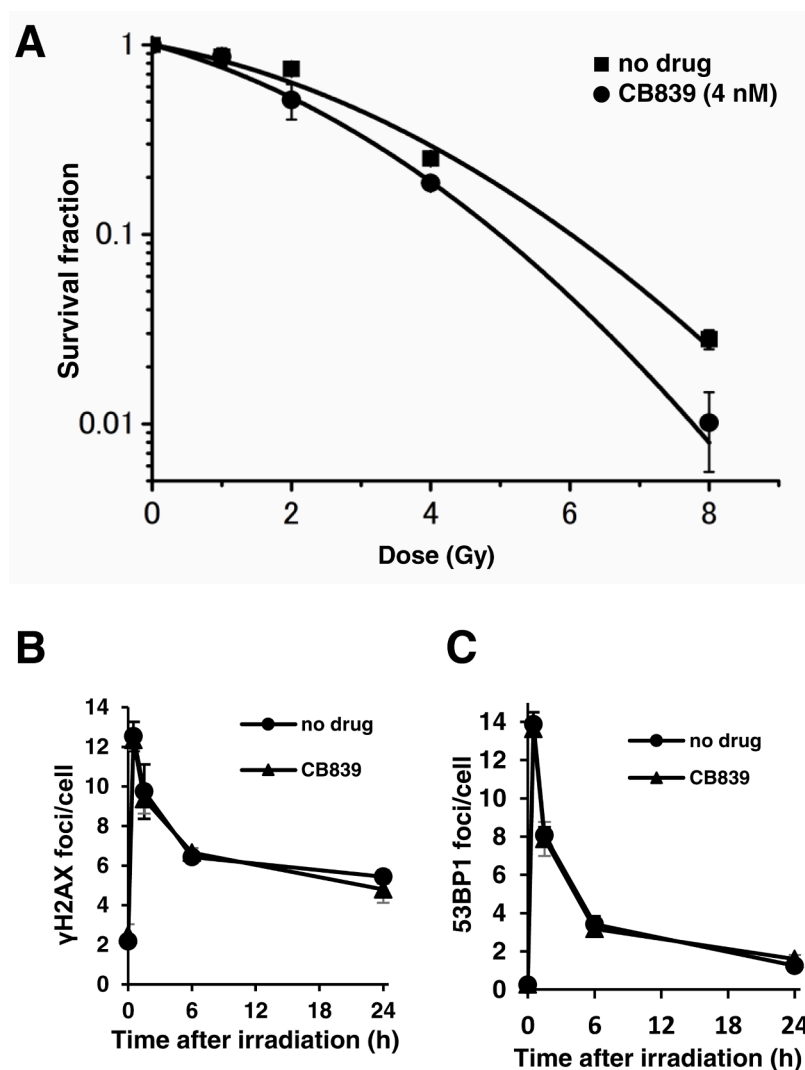


Fig. 1. The effect of the GLS inhibitor CB839 on radiosensitivity and radiation-induced DNA damage in A549 cells. (A) The clonogenic survival of A549 cells after treatment with CB839 and X-irradiation was assessed in the colony formation assay. A549 cells were treated with 4 nM CB839 immediately after X-irradiation, and then incubated for 14 days. Radiation-induced DNA damage was evaluated by immunostaining for γH2AX (B) and 53BP1 (C). The cells were seeded and incubated overnight. The cells were treated with (\blacktriangle) or without (\bullet) 10 nM CB839 immediately after X-irradiation (0.5 Gy (B) or 1 Gy (C)) and incubated for 0, 0.5, 1, 6, or 24 h. Data are expressed as mean \pm SD for three experiments.

mitochondrial ETC is essential for cell survival, and CB839 enhances radiosensitivity by inhibiting this activation, but DNA damage and the DNA repair capability do not contribute to CB839-induced radiosensitization.

Inhibition of glutaminolysis enhanced radiation-induced senescence

GLS inhibition was reported to induce senescence in pancreatic cancer cell lines [15]. X-irradiation increased the percentage of SA- β -gal-positive cells; furthermore, CB839 treatment after X-irradiation increased the percentage of SA- β -gal-positive A549 cells from 10.5% to 24.8% (Fig. 2A). Inhibition of glutamine-related metabolic pathways by treatment of low-glutamine medium also significantly increased percentage of SA- β -gal positive A549 and H460 cells after X-irradiation (Figs. 2B and S5A). The secretion of SASP factors is known to be increased in senescent cells [24]. We evaluated the concentrations of IL-6 and IL-8 secreted from cancer cells into the medium. The combination of treatment with CB839 or 0.5 mM glutamine medium and X-irradiation significantly increased IL-6 and IL-8 secretion in A549 cells and H460 cells compared with that achieved using X-irradiation alone (Figs. 2C, 2D, 2E, 2F, S5B and S5C). These results revealed that radiation-induced senescence is enhanced by the inhibition of glutaminolysis. The effect of glutaminolysis inhibition on radiation-induced apoptosis was determined by flow cytometry with annexin-V/PI staining. While X-irradiation increased the percentage of cells showing early apoptosis, number of these apoptotic cells against total cells was

remained considerably low. The percentages of early apoptotic, late apoptotic, and necrotic A549 cells after X-irradiation were unaffected by CB839 treatment (Figs. 3A, 3B, and 3C), indicating that glutaminolysis inhibition did not enhance apoptosis or necrosis after X-irradiation. These results suggested that senescence contributes to radiosensitization by glutaminolysis inhibition, whereas apoptosis or necrosis do not.

Treatment with low-glutamine medium decreased the expression of p-CDK2, cyclin A, and cyclin B1 after X-irradiation

We next investigated the molecular mechanism underlying the enhancement of radiation-induced cellular senescence in response to low-glutamine medium. The effect of treatment with low glutamine medium after X-irradiation on p53 and p21 expression was determined. The expression of p53 and p21 increased 10 h after X-irradiation, and the levels were maintained until 96 h. Combined treatment with a low-glutamine medium and X-irradiation did not alter the expression of p53 and p21 from that achieved with only X-irradiation until 24 h, but the expression of p53 and p21 after 48 h of combined treatment was lower than that obtained with only X-irradiation (Fig. 4A). These results indicated that p53 and p21 do not directly contribute to the enhancement of radiation-induced senescence by treatment with low-glutamine medium. To evaluate the mechanism underlying cell cycle arrest induced by treatment with low-glutamine medium, we assessed the phosphorylation of CDK2 and the expression of cyclin A and cyclin B1. Cyclin A and CDK2 form cyclin A-CDK2 complexes and regulate the G₁/S

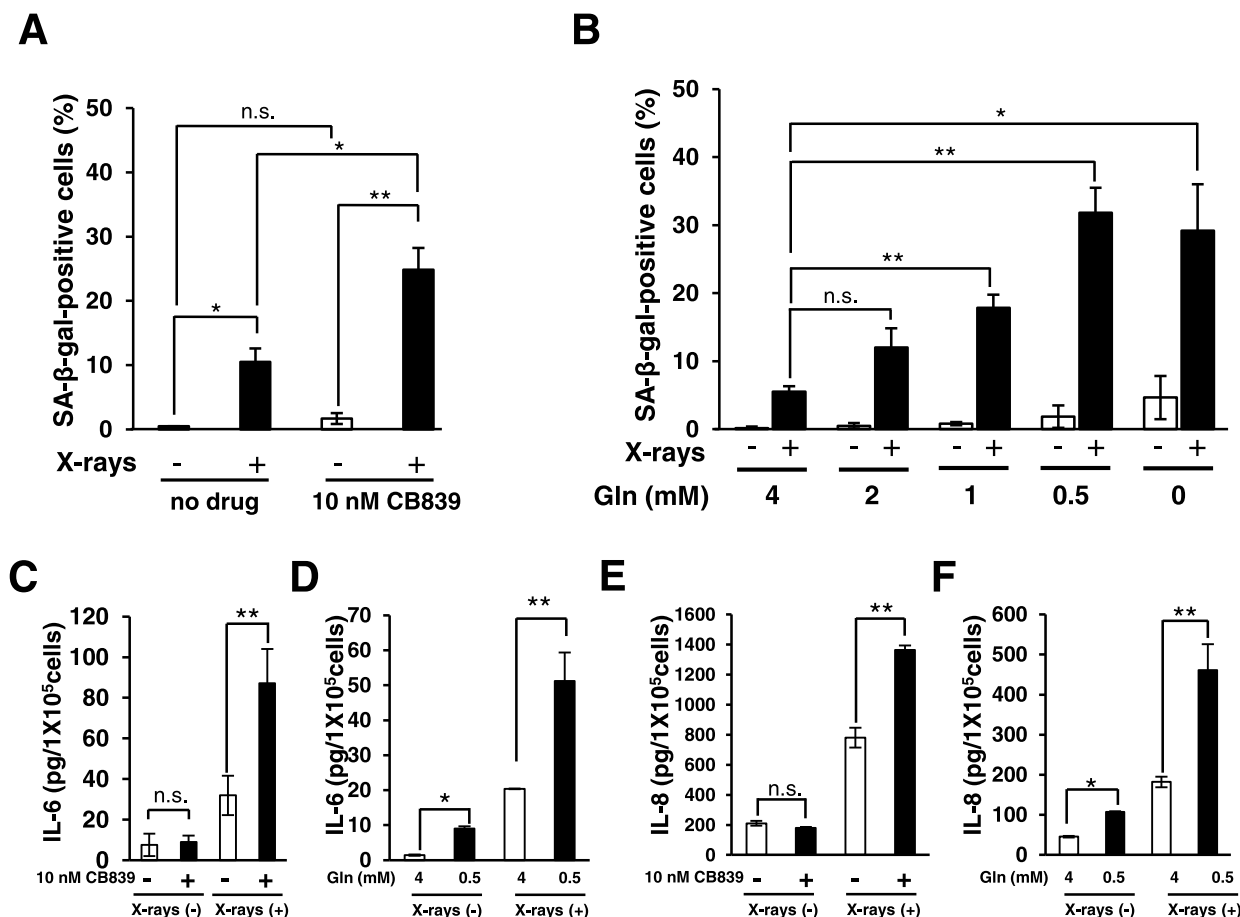


Fig. 2. The effect of glutaminolysis inhibition on radiation-induced senescence in A549 cells. (A, B) Senescence-associated beta galactosidase (SA- β -gal) staining was performed 5 days after X-irradiation (5 Gy). Treatment with 10 nM CB839 (A) or low-glutamine (0, 0.5, 1, or 2 mM) medium (B) was performed immediately after X-irradiation. Enzyme-linked immunosorbent assay for IL-6 (C, D) and IL-8 (E, F) was performed 5 days after X-irradiation (5 Gy). Treatment with 10 nM CB839 (C, E) or 0.5 mM glutamine medium (D, F) was performed immediately after X-irradiation. Data are expressed as means \pm SD for three experiments. * p <0.05, ** p <0.01, significant difference, n.s., not significant.

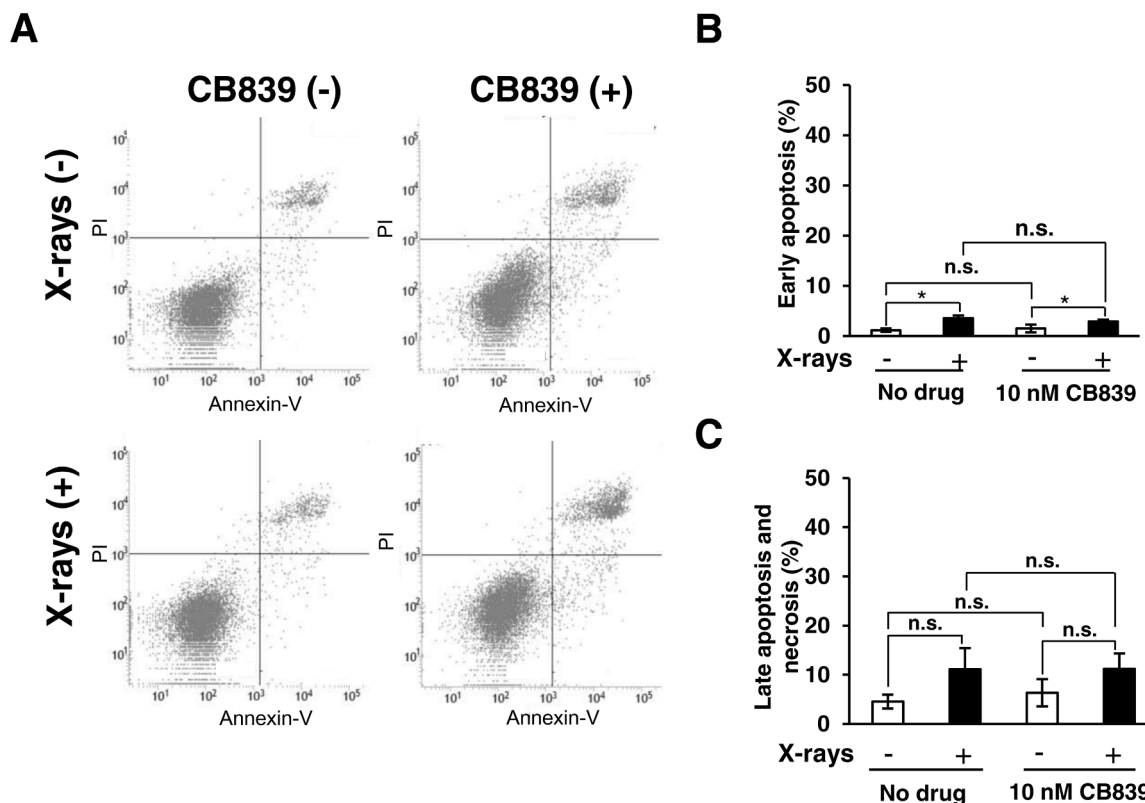


Fig. 3. The effect of glutaminolysis inhibition on radiation-induced apoptosis and necrosis. (A-C) Apoptosis and necrosis were analyzed by flow cytometry for annexin-V /propidium iodide detection. (A) Representative plot was shown. Annexin-V single positive cells were considered early apoptotic cells (B), and annexin-V and PI double positive cells were considered late apoptosis and necrosis (C). Flow cytometry was performed 3 days after X-irradiation (5 Gy). Ten nanomolar CB839 was administered immediately after X-irradiation. Data are expressed as means \pm SD for three experiments. * $p < 0.05$, significant difference, n.s., not significant.

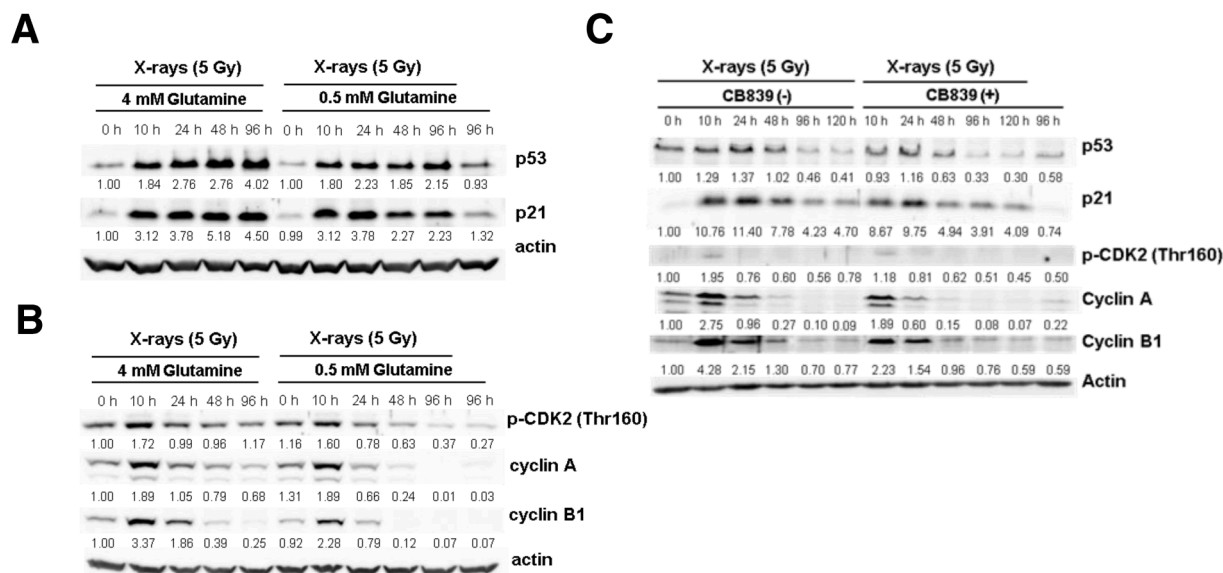


Fig. 4. Effect of treatment with low-glutamine medium or CB839 on the expression of p53, p21, p-CDK2, cyclin A, and cyclin B1. (A, B) Samples of western blotting for p53, p21 (A), p-CDK2, cyclin A, and cyclin B1 (B) were collected at 0, 10, 24, 48, and 96 h after X-irradiation (5 Gy) and/or treatment with low-glutamine medium. (C) Samples of western blotting for p53, p21, p-CDK2, cyclin A, and cyclin B1 were collected at 0, 10, 24, 48, 96, and 120 h after X-irradiation (5 Gy) and/or treatment with 10 nM CB839. Incubation in 0.5 mM glutamine medium or 10 nM CB839 was performed immediately after X-irradiation.

phase transition [44]. Cyclin B1 forms complexes with CDK1 and promotes the G₂/M phase transition. Reportedly, CDK2 expression decreases in senescent cells [45]. Cyclin A and cyclin B1 levels are also reduced during DNA damage-induced senescence [46]. In contrast to

glutamine medium of normal concentration, low-glutamine medium reduced the levels of p-CDK2, cyclin A, and cyclin B1 at 24 h after X-irradiation (Fig. 4B). Similar to treatment with low glutamine medium, CB839 treatment decreased the level of p53, p21, p-CDK2, cyclin

A and cyclin B1 after X-irradiation (Fig. 4C). These results suggested that decreased CDK2 and cyclin A/B1 expression may be related to senescence-like cell cycle arrest enhanced by glutamine shortage in X-irradiated A549 cells, although the increase in the proportion of senescent cells in response to glutamine shortage is independent of the functions of p53 and p21.

ABT263, a senolytic drug, induced apoptosis in radiation-exposed senescent cells

To determine the sublethal dose of ABT263 appropriate for use in the experiment, we analyzed the cytotoxicity of ABT263 alone. Treatment with 5 μM or 10 μM ABT263 exerted limited effect on cell survival and proliferation, whereas treatment with 20 μM ABT263 induced clear cytotoxic effects in A549 cells (Fig. 5A). Administration of 2.5 μM or 5 μM ABT263 had little effect on cell survival and proliferation in H460 cells (Fig. S6A). Therefore, 2.5 μM ABT263 was administered to evaluate the effect of ABT263 on apoptosis or senescence induced by treatment with low-glutamine medium and/or X-irradiation in both cells. We

assessed the effects of ABT263 treatment on radiation-induced senescence, which was enhanced by glutamine shortage. ABT263 treatment did not affect the rate of proliferation of SA- β -gal-positive cells in the absence of X-irradiation (Fig. 5B). In A549 cells, ABT263 treatment after X-irradiation significantly decreased the rate of senescence from approximately 13.0% to approximately 1.83%; furthermore, it significantly decreased the rate of senescence from approximately 39.0% to approximately 6.83% when combined with treatment with low-glutamine medium and X-irradiation (Fig. 5B). Similarly, ABT263 decreased the rate of senescent cells after X-irradiation or the combination of treatment with low-glutamine medium and X-irradiation in H460 cells (Fig. S6B). Concurrently, ABT263 significantly decreased the secretion of IL-6 (Figs. 5C and S6C) and IL-8 (Figs. 5D and S6D) from A549 and H460 cells when administered after X-irradiation or after glutamine shortage combined with X-irradiation. ABT263 treatment after X-irradiation increased the rate of early apoptosis of A549 and H460 cells, and the combination of low-glutamine medium and ABT263 treatment after X-irradiation increased the rate of early apoptosis, compared to that obtained after treatment with glutamine medium of

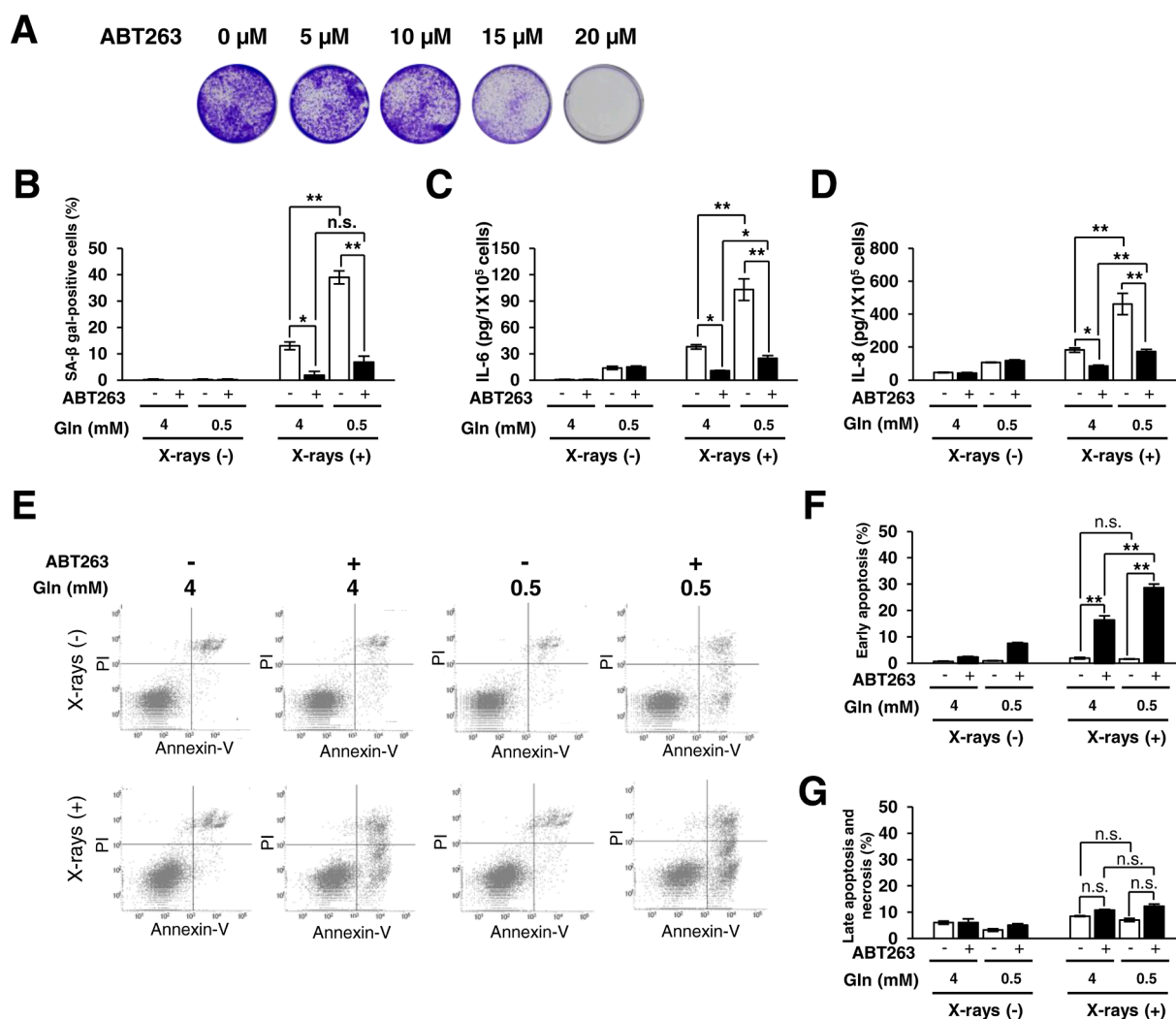


Fig. 5. The effect of the senolytic drug ABT263 on radiation-induced senescence, apoptosis, and necrosis. (A) Cytotoxicity to ABT263 in A549 cells was analyzed by crystal violet staining. The cells were seeded and incubated overnight. After incubation, the cells were treated with 5, 10, 15, or 20 μM ABT263 and incubated for 5 days. (B, C) Senescence-associated beta galactosidase (SA- β -gal) staining (B) and enzyme-linked immunosorbent assay for IL-6 (C) and IL-8 (D) was performed 5 days after X-irradiation (5 Gy). Cells were treated with 2.5 μM ABT263 and/or 0.5 mM glutamine medium immediately after X-irradiation. (E-G) Apoptosis and necrosis were analyzed by flow cytometry for annexin-V /propidium iodide detection. (E) Representative plot was shown. Annexin-V single positive cells were considered early apoptotic cells (F), and annexin-V and PI double positive cells were considered late apoptotic and necrotic cells (G). Flow cytometry was performed 3 days after X-irradiation (5 Gy). Cells were treated with 2.5 μM ABT263 and/or 0.5 mM glutamine medium immediately after X-irradiation. Data are expressed as means \pm SD for three experiments. * $p < 0.05$, ** $p < 0.01$, significant difference, n.s., not significant.

normal concentration (Figs. 5F and S6F). These data show that ABT263 treatment and the combination of glutamine shortage and ABT263 treatment considerably enhanced radiation-induced apoptosis; moreover, ABT263 treatment also increased radiation-induced late apoptosis and necrosis. However, the degree of increase was small, and glutamine medium of low concentration did not affect radiation-induced late apoptosis and necrosis in A549 and H460 cells (Figs. 5G and S6G). These results suggest that ABT263 improves the efficacy of radiation cancer therapy by inducing apoptosis in senescent cancer cells.

Discussion

Since glutaminolysis is essential for energy metabolism and biomolecule synthesis in several cancer cell types [6], glutaminolysis has been studied as a target for cancer therapy [1,8,9,11,15]. Glutaminolysis inhibition suppresses growth or survival and enhances radiosensitivity in some cancer cell lines [11]. In this study, the phenotype of cell death induced by X-irradiation with and without glutaminolysis inhibitors was characterized, and the relationship between energy metabolism and cell death after these treatments was also investigated in non-small cell lung cancer cell lines.

Glutamate synthesis, mitochondrial oxygen consumption, and ATP production were enhanced in A549 cells subjected to X-irradiation (Fig. S1). The increase was inhibited by the GLS inhibitor CB839, suggesting that the radiation-induced enhancement of ATP production through mitochondrial ETC is highly dependent on glutaminolysis in A549 cells. These findings suggested that there exists a strong correlation between the inhibition of intracellular energy production by glutaminolysis and the radiosensitization effect shown in Fig. 1. A previous study conducted in our laboratory showed that a mitochondrial ETC inhibitor suppressed ATP production and induced radiosensitization in human cervical adenocarcinoma HeLa cells and A549 cells [39]. Qin et al. reported that the increase in ATP production after X-irradiation is a radioadaptive response, and the excess ATP produced is used to effectively mitigate DNA damage [47]. These data indicate that the enhancement of glutamine-dependent energy metabolism is necessary for cell survival after X-irradiation, and CB839 treatment enhances radiosensitivity by decreasing glutamine-dependent ATP production.

Glutaminolysis inhibition has been reported to induce senescence in pancreatic cancer cells [15] and endothelial cells [48]; however, it remains unclear whether senescence contributes to radiosensitization and chemosensitization by glutaminolysis inhibition. In the SA- β -gal assay (Figs. 2A, 2B and S5A) and flow cytometry experiment with annexin-V/PI staining (Fig. 3), we showed that glutaminolysis inhibition after X-irradiation enhanced senescence, but not apoptosis. These results suggest that cellular senescence primarily contributes to radiosensitization by glutaminolysis inhibition. Senescent cells are characterized by the increased expression/activity of several markers, such as SA- β -gal and cell cycle inhibitors (including p53, p21, and p16), and the increased secretion of SASP factors. In this study, glutaminolysis inhibition increased the rate of SA- β -gal-positive cell proliferation and IL-6 secretion after X-irradiation (Fig. 2 and S5). However, the increase in p53 and p21 expression in response to the combination of low-glutamine medium treatment and X-irradiation was less than that obtained with X-irradiation alone (Fig. 4A). These observations suggest that the enhancement of radiation-induced senescence by glutamine shortage may be independent of p53 and p21. The MKK3/6-p38 δ MAPK pathway was reported as a senescence pathway independent of p53, p21, and p16 [25]. Furthermore, Cipriano et al. showed that Ras-induced senescence mediated by the activation of the TGF- β receptor does not require p53, p21, or p16 [49]. TGF- β , which is associated with glutaminolysis, promotes GLS expression [50]. Since the relationship between radiation-induced senescence enhanced by glutamine shortage and p53-, p21-, and p16-independent cellular senescence remains unclear, further studies involving p38 δ , TNF- β , and Ras are required to elucidate the mechanism underlying the increase in cellular senescence induced

by irradiation with the inhibition of glutaminolysis. Next, with respect to the relationship between the CDK/cyclin system and senescence-like cell cycle arrest, the expression of CDK2 has been reported to decrease in senescent human umbilical vein endothelial cells [46], and cyclin A and cyclin B1 levels have been shown to be decreased in DNA damage-induced senescence in HeLa cells [30]. These findings indicate that the CDK/cyclin system plays a major role in senescence-like cell cycle arrest. As shown in Fig. 4B, the expression of cyclin A, cyclin B, and p-CDK2 after irradiation and treatment with 4 mM glutamine was significantly lower than that obtained after irradiation and treatment with 0.5 mM glutamine. These results suggest that in the present study, the low expression of cyclin A, cyclin B1, and CDK2 after irradiation under glutaminolysis inhibitory conditions may have been related to the enhancement of radiation-induced senescence-like cell cycle arrest.

Senescent cells secrete SASP factors, such as cytokines, chemokines, growth factors, and proteases, which exert negative effects. The combination of glutaminolysis inhibition and X-irradiation induced the secretion of IL-6 and IL-8 with generation of SA- β -gal-positive cells (Figs. 2C, 2D, 2E, 2F and S5). Reportedly, MPM cells induced EMT and acquired chemoresistance to pemetrexed when treated with the conditioned medium of senescent MPM cells producing SASP factors [30]. Inflammatory cytokines cause chronic inflammation and stimulate cancer proliferation by promoting angiogenesis [35]. Since the presence of senescent cells can cause these negative effects, the elimination of senescent cancer cells is beneficial for cancer therapy. Therefore, senolytic drugs that induce apoptosis in senescent cells are garnering increasing attention [34]. ABT263 disrupts Bcl-2/Bcl-X_L interference and initiates apoptosis [33]. Reportedly, combined treatment with ABT263 and doxorubicin or etoposide induces apoptosis and decreases senescence compared to that observed upon treatment with only doxorubicin or etoposide in MDA-MB-231 and A549 cells [33]. In this study, ABT263 increased the number of apoptotic cells and decreased the number of senescent cells obtained after X-irradiation. Moreover, ABT263 treatment administered in combination with treatment with low-glutamine medium increased apoptosis and decreased senescence compared to that obtained with ABT263 treatment after X-irradiation (Figs. 5 and S6). These results suggest that combination treatment with senolytic drugs and X-irradiation under glutamine shortage is useful for the development of a novel cancer therapy without side effects such as inflammation and metastasis.

In summary, the present study demonstrated that glutaminolysis-dependent ATP production was increased by X-irradiation, and the GLS inhibitor CB839 enhanced radiosensitivity by suppressing the increase in ATP production. Furthermore, enhanced radiation-induced senescence, which can be independent of p53 and p21, primarily contributes to radiosensitization by glutaminolysis inhibition. Lastly, treatment with senolytic drugs increased the transformation of radiation-induced senescent cells to apoptotic cells. These data indicate that senolytic drugs may improve the efficacy of cancer radiation therapy by inhibiting its side effects.

Funding

This work was supported by JSPS KAKENHI Grant Numbers 19H04263, 19K22586 [HY], 22KKO250, and 20H00443 [OI].

CRedit authorship contribution statement

Masaki Fujimoto: Methodology, Investigation, Visualization, Writing – original draft. **Ritsuko Higashiyama:** Methodology, Investigation. **Hironobu Yasui:** Supervision, Funding acquisition, Writing – review & editing. **Koya Yamashita:** Investigation, Data curation. **Osamu Inanami:** Conceptualization, Project administration, Resources, Funding acquisition, Writing – review & editing.

Declaration of Competing Interests

The authors declare that they have no known competing financial interests or personal relationships that could have influenced the work reported in this paper

Acknowledgments

The authors deeply appreciate the technical support of MR. Koichi Ozaki in the flow cytometry experiments in this study. We would like to also thank Editage (www.editage.com) for English language editing.

Supplementary materials

Supplementary material associated with this article can be found, in the online version, at doi:[10.1016/j.tranon.2022.101431](https://doi.org/10.1016/j.tranon.2022.101431).

References

- J. Son, C.A. Lyssiotis, H. Ying, X. Wang, S. Hua, M. Ligorio, R.M. Perera, C. R. Ferrone, E. Mullarky, N. Shyh-Chang, Y. Kang, J.B. Fleming, N. Bardeesy, J. M. Asara, M.C. Haigis, R.A. Depinho, L.C. Cantley, A.C. Kimmelman, Glutamine supports pancreatic cancer growth through a KRAS-regulated metabolic pathway, *Nature* 496 (2013) 101–105, <https://doi.org/10.1038/nature12040>.
- A. Galan-Cobo, P. Sitthideatphaiboon, X. Qu, A. Poteete, M.A. Pisegna, P. Tong, P. H. Chen, L.K. Boroughs, M.L.M. Rodriguez, W. Zhang, F. Parlati, J. Wang, V. Gandhi, F. Skoulidis, R.J. DeBerardinis, J.D. Minna, J.v. Heymach, LKB1 and KEAP1/NRF2 pathways cooperatively promote metabolic reprogramming with enhanced glutamine dependence in KRAS-mutant lung adenocarcinoma, *Cancer Res.* 79 (2019) 3251–3267, <https://doi.org/10.1158/0008-5472.CAN-18-3527>.
- K. Thangavelu, C.Q. Pan, T. Karlberg, G. Balaji, M. Uttamchandani, V. Suresh, H. Schüler, B.C. Low, J. Sivaraman, Structural basis for the allosteric inhibitory mechanism of human kidney-type glutaminase (KGA) and its regulation by Raf-Mek-Erk signaling in cancer cell metabolism, *Proc. Natl. Acad. Sci. USA* 109 (2012) 7705–7710, <https://doi.org/10.1073/pnas.1116573109>.
- P. Gao, I. Tchernyshyov, T.C. Chang, Y.S. Lee, K. Kita, T. Ochi, K.I. Zeller, A.M. de Marzo, J.E. van Eyk, J.T. Mendell, C.v. Dang, C-Myc suppression of miR-23a/b enhances mitochondrial glutamine expression and glutamine metabolism, *Nature* 458 (2009) 762–765, <https://doi.org/10.1038/nature07823>.
- M.I. Gross, S.D. Demo, J.B. Dennison, L. Chen, T. Chernov-Rogan, B. Goyal, J. R. Janes, G.J. Laidig, E.R. Lewis, J. Li, A.L. MacKinnon, F. Parlati, M.L. M. Rodriguez, P.J. Shwonek, E.B. Sjogren, T.F. Stanton, T. Wang, J. Yang, F. Zhao, M.K. Bennett, Antitumor activity of the glutaminase inhibitor CB-839 in triple-negative breast cancer, *Mol. Cancer Ther.* 13 (2014) 890–901, <https://doi.org/10.1158/1535-7163.MCT-13-0870>.
- L. Jin, G.N. Alesi, S. Kang, Glutaminolysis as a target for cancer therapy, *Oncogene* 35 (2016) 3619–3625, <https://doi.org/10.1038/ncr.2015.447>.
- J.M. Matés, F.J. di Paola, J.A. Campos-Sandoval, S. Mazurek, J. Márquez, Therapeutic targeting of glutaminolysis as an essential strategy to combat cancer, *Semin. Cell Dev. Biol.* 98 (2020) 34–43, <https://doi.org/10.1016/j.semcdb.2019.05.012>.
- M. Hassanein, M.D. Hoeksema, M. Shiota, J. Qian, B.K. Harris, H. Chen, J.E. Clark, W.E. Alborn, R. Eisenberg, P.P. Massion, SLC1A5 mediates glutamine transport required for lung cancer cell growth and survival, *Clin. Cancer Res.* 19 (2013) 560–570, <https://doi.org/10.1158/1078-0432.CCR-12-2334>.
- Q. Wang, K.A. Beaumont, N.J. Otte, J. Font, C.G. Bailey, M. van Geldermalsen, D. M. Sharp, J.C. Tiffen, R.M. Ryan, M. Jormakka, N.K. Haass, J.E.J. Rasko, J. Holst, Targeting glutamine transport to suppress melanoma cell growth, *Int. J. Cancer* 135 (2014) 1060–1071, <https://doi.org/10.1002/ijc.28749>.
- L. Yang, S. Venneti, D. Nagrath, Glutaminolysis: A hallmark of cancer metabolism, *Annu. Rev. Biomed. Eng.* 19 (2017) 163–194, <https://doi.org/10.1146/annurev-bioeng-071516-044546>.
- D.R. Sappington, E.R. Siegel, G. Hiatt, A. Desai, R.B. Penney, A. Jamshidi-Parsian, R.J. Griffin, G. Boysen, Glutamine drives glutathione synthesis and contributes to radiation sensitivity of A549 and H460 lung cancer cell lines, *Biochim. Biophys. Acta.* 1860 (2016) 836–843, <https://doi.org/10.1016/j.bbagen.2016.01.021>.
- C.P. Masamba, P. LaFontaine, Molecular targeting of glutaminase sensitizes ovarian cancer cells to chemotherapy, *J. Cell Biochem.* 119 (2018) 6136–6145, <https://doi.org/10.1002/jcb.26814>.
- L. Yuan, X. Sheng, L.H. Clark, L. Zhang, H. Guo, H.M. Jones, A.K. Willson, P. A. Gehrig, C. Zhou, V.L. Bae-Jump, Glutaminase inhibitor compound 968 inhibits cell proliferation and sensitizes paclitaxel in ovarian cancer, *Am. J. Transl. Res.* 8 (2016) 4265–4277.
- K. Valter, L. Chen, B. Kruspig, P. Maximchik, H. Cui, B. Zhivotovsky, V. Gogvadze, Contrasting effects of glutamine deprivation on apoptosis induced by conventionally used anticancer drugs, *Biochim. Biophys. Acta.* 1864 (2017) 498–506, <https://doi.org/10.1016/j.bbamcr.2016.12.016>.
- S. Yang, S. Hwang, M. Kim, S. Bin Seo, J.H. Lee, S.M. Jeong, Mitochondrial glutamine metabolism via GOT2 supports pancreatic cancer growth through senescence inhibition article, *Cell Death Dis* 9 (2018), 55, <https://doi.org/10.1038/s41419-017-0089-1>.
- P. Jiang, W. Du, A. Mancuso, K.E. Wellen, X. Yang, Reciprocal regulation of p53 and malic enzymes modulates metabolism and senescence, *Nature* 493 (2013) 689–693, <https://doi.org/10.1038/nature11776>.
- J. Kaplon, L. Zheng, K. Meissl, B. Chaneton, V.A. Selivanov, G. MacKay, S.H. van der Burg, E.M.E. Verdegaaal, M. Cascante, T. Shlomi, E. Gottlieb, D.S. Peepker, A key role for mitochondrial gatekeeper pyruvate dehydrogenase in oncogene-induced senescence, *Nature* 498 (2013) 109–112, <https://doi.org/10.1038/nature12154>.
- M. Petit, R. Kozziel, S. Etamad, H. Pircher, P. Jansen-Dürr, Depletion of oxaloacetate decarboxylase FAHD1 inhibits mitochondrial electron transport and induces cellular senescence in human endothelial cells, *Exp. Gerontol.* 92 (2017) 7–12, <https://doi.org/10.1016/j.exger.2017.03.004>.
- J. Sabbatinelli, F. Prattichizzo, F. Olivieri, A.D. Procopio, M.R. Rippo, A. Giuliani, Where metabolism meets senescence: focus on endothelial cells, *Front. Physiol.* 18 (2019), <https://doi.org/10.3389/fphys.2019.01523>.
- L. Hayflick, P.S. Moorhead, The serial cultivation of human diploid cell strains, *Exp. Cell Res.* 25 (1961) 585–621, [https://doi.org/10.1016/0014-4827\(61\)90192-6](https://doi.org/10.1016/0014-4827(61)90192-6).
- X. ling Liu, J. Ding, L-H. Meng, Oncogene-induced senescence: a double edged sword in cancer., *Acta Pharmacol. Sin.* 39 (2018) 1553–1558, <https://doi.org/10.1038/aps.2017.198>.
- D. Eriksson, T. Stigbrand, Radiation-induced cell death mechanisms, *Tumor Biol.* 31 (2010) 363–372, <https://doi.org/10.1007/s13277-010-0042-8>.
- A. Calcinotto, J. Kohli, E. Zagato, L. Pellegrini, M. Demaria, A. Alimonti, Cellular senescence: aging, cancer, and injury, *Physiol. Rev.* 99 (2019) 1047–1078, <https://doi.org/10.1152/physrev.00020.2018>.
- B.G. Childs, D.J. Baker, J.L. Kirkland, J. Campisi, J.M. Deursen, Senescence and apoptosis: dueling or complementary cell fates? *EMBO Rep.* 15 (2014) 1139–1153, <https://doi.org/10.15252/embr.201439245>.
- J. Kwong, M. Chen, D. Lv, N. Luo, W. Su, R. Xiang, P. Sun, Induction of p38 β expression plays an essential role in oncogenic ras-induced senescence, *Mol. Cell Biol.* 33 (2013) 3780–3794, <https://doi.org/10.1128/MCB.00784-13>.
- Y. Xu, N. Li, R. Xiang, P. Sun, Emerging roles of the p38 MAPK and PI3K/AKT/mTOR pathways in oncogene-induced senescence, *Trends Biochem. Sci.* 39 (2014) 268–276, <https://doi.org/10.1016/j.tibs.2014.04.004>.
- B. Wang, J. Kohli, M. Demaria, Senescent cells in cancer therapy: Friends or foes? *Trends Cancer* 6 (2020) 838–857, <https://doi.org/10.1016/j.trecan.2020.05.004>.
- E. Mavrogonatou, H. Pratsinis, D. Kletsas, The role of senescence in cancer development, *Semin. Cancer Biol.* 62 (2020) 182–191, <https://doi.org/10.1016/j.semcancer.2019.06.018>.
- A.R. Davalos, J-P. Coppe, J. Campisi, P-Y. Desprez, Senescent cells as a source of inflammatory factors for tumor progression, *Cancer Metastasis Rev.* 29 (2010) 273–283, <https://doi.org/10.1007/s10555-010-9220-9>.
- C. Canino, F. Mori, A. Cambria, A. Diamantini, S. Germoni, G. Alessandrini, G. Borsellino, R.Z. Galati, L. Battistini, R. Blandino, F. Facciolo, G. Citro, S. Strano, P. Muti, G. Blandino, M. Cioce, SASP mediates chemoresistance and tumor-initiating-activity of mesothelioma cells, *Oncogene* 31 (2012) 3148–3163, <https://doi.org/10.1038/ncr.2011.485>.
- R-M. Labeerge, Y. Sun, A.v. Orjalo, C.K. Patil, A. Freund, L. Zhou, S.C. Curran, A. R. Davalos, K.A. Wilson-Edell, S. Liu, C. Limbad, M. Demaria, P. Li, G.B. Hubbard, Y. Ikeno, M. Javors, P-Y. Desprez, C.C. Benz, P. Kapahi, P.S. Nelson, J. Campisi, MTOR regulates the pro-tumorigenic senescence-associated secretory phenotype by promoting IL1A translation, *Nature Cell Biol.* 17 (2015) 1049–1061, <https://doi.org/10.1038/ncb3195>.
- P. Ortiz-Montero, A. Londoño-Vallejo, J-P. Vernot, Senescence-associated IL-6 and IL-8 cytokines induce a self- and cross-reinforced senescence/inflammatory milieu strengthening tumorigenic capabilities in the MCF-7 breast cancer cell line, *Cell Commun. Signal* 15 (17) (2017), <https://doi.org/10.1186/s12964-017-0172-3>.
- T. Saleh, V.J. Carpenter, L. Tyutyunyk-Massey, G. Murray, J.D. Levenson, A. J. Souers, M.R. Alotaibi, A.C. Faber, J. Reed, H. Harada, D.A. Gewirtz, Clearance of therapy-induced senescent tumor cells by the senolytic ABT-263 via interference with BCL-XL–BAX interaction, *Mol. Oncol.* 14 (2020) 2504–2519, <https://doi.org/10.1002/1878-0261.12761>.
- C. Tse, A.R. Shoemaker, J. Adickes, M.G. Anderson, J. Chen, S. Jin, E.F. Johnson, K. C. Marsh, M.J. Mitten, P. Nimicker, L. Roberts, S.K. Tahir, Y. Xiao, X. Yang, H. Zhang, S. Fesik, S.H. Rosenberg, S.W. Elmore, ABT-263: a potent and orally bioavailable Bcl-2 family inhibitor, *Cancer Res.* 68 (2008) 3421–3428, <https://doi.org/10.1158/0008-5472.CAN-07-5836>.
- S. Short, E. Fielder, S. Miwa, T. von Zglinicki, Senolytics and senostatics as adjuvant tumour therapy, *EBioMedicine* 41 (2019) 683–692, <https://doi.org/10.1016/j.ebiom.2019.01.056>.
- A.A. Mongin, M.C. Hyzinski-García, M.Y. Vincent, R.W. Keller, A simple method for measuring intracellular activities of glutamine synthetase and glutaminase in glial cells Mongin AA, Hyzinski-García MC, Vincent MY, Keller RW Jr. A simple method for measuring intracellular activities of glutamine synthetase and glutaminase in glial cells, *Am. J. Physiol. Cell Physiol.* 301 (2011) 814–822, doi:[10.1152/ajpcell.00035.2011](https://doi.org/10.1152/ajpcell.00035.2011).
- K. Yamamoto, H. Yasui, T. Bo, T. Yamamori, W. Hiraoka, T. Yamasaki, K. ichi Yamada, O. Inanami, Genotoxic responses of mitochondrial oxygen consumption rate and mitochondrial semiquinone radicals in tumor cells, *Appl. Magn. Reson.* 49 (2018) 837–851, <https://doi.org/10.1007/s00723-018-1007-0>.
- K. Yamamoto, Y. Ikenaka, T. Ichise, T. Bo, M. Ishizuka, H. Yasui, W. Hiraoka, T. Yamamori, O. Inanami, Evaluation of mitochondrial redox status and energy metabolism of X-irradiated HeLa cells by LC/UV, LC/MS/MS and ESR, *Free Radic. Res.* 52 (2018) 648–660, <https://doi.org/10.1080/10715762.2018.1460472>.

- [39] H. Yasui, K. Yamamoto, M. Suzuki, Y. Sakai, T. Bo, M. Nagane, E. Nishimura, T. Yamamori, T. Yamasaki, K. Ichi Yamada, O. Inanami, Lipophilic triphenylphosphonium derivatives enhance radiation-induced cell killing via inhibition of mitochondrial energy metabolism in tumor cells, *Cancer Lett.* 390 (2017) 160–167, <https://doi.org/10.1016/j.canlet.2017.01.006>.
- [40] T. Yamamori, H. Yasui, M. Yamazumi, Y. Wada, Y. Nakamura, H. Nakamura, O. Inanami, Ionizing radiation induces mitochondrial reactive oxygen species production accompanied by upregulation of mitochondrial electron transport chain function and mitochondrial content under control of the cell cycle checkpoint, *Free Radic. Biol. Med.* 53 (2012) 260–270, <https://doi.org/10.1016/j.freeradbiomed.2012.04.033>.
- [41] C. Diepart, J. Verrax, P.B. Calderon, O. Feron, B.F. Jordan, B. Gallez, Comparison of methods for measuring oxygen consumption in tumor cells in vitro, *Anal. Biochem.* 396 (2010) 250–256, <https://doi.org/10.1016/j.ab.2009.09.029>.
- [42] N. Li, K. Ragheb, G. Lawler, J. Sturgis, B. Rajwa, J.A. Melendez, J.P. Robinson, Mitochondrial complex I inhibitor rotenone induces apoptosis through enhancing mitochondrial reactive oxygen species production, *J. Biol. Chem.* 278 (2003) 8516–8525, <https://doi.org/10.1074/jbc.M210432200>.
- [43] T. Deguchi, K. Hosoya, S. Kim, Y. Murase, K. Yamamoto, T. Bo, H. Yasui, O. Inanami, M. Okumura, Metformin preferentially enhances the radio-sensitivity of cancer stem-like cells with highly mitochondrial respiration ability in HMPOS, *Mol. Ther. Oncolytics* 22 (2021) 143–151, <https://doi.org/10.1016/j.omto.2021.08.007>.
- [44] C.H. Yam, T.K. Fung, R.Y.C. Poon, Cyclin A in cell cycle control and cancer, *Cell. Mol. Life Sci.* 59 (2002) 1317–1326, <https://doi.org/10.1007/s00018-002-8510-y>.
- [45] D.A. Freedman, J. Folkman, CDK2 translational down-regulation during endothelial senescence, *Exp. Cell Res.* 307 (2005) 118–130, <https://doi.org/10.1016/j.yexcr.2005.03.025>.
- [46] I. Kikuchi, Y. Nakayama, T. Morinaga, Y. Fukumoto, N. Yamaguchi, A decrease in cyclin B1 levels leads to polyploidization in DNA damage-induced senescence, *Cell Biol. Int.* 34 (2010) 645–653, <https://doi.org/10.1042/CBI20090398>.
- [47] L. Qin, M. Fan, D. Candas, G. Jiang, S. Papadopoulos, L. Tian, G. Woloschak, D.J. J. Grdina, J.J.J. Li, CDK1 Enhances Mitochondrial Bioenergetics for radiation-induced DNA repair, *Cell Rep.* 13 (2015) 2056–2063, <https://doi.org/10.1016/j.celrep.2015.11.015>.
- [48] H. Unterluggauer, S. Mazurek, B. Lener, E. Hütter, E. Eigenbrodt, W. Zwerschke, P. Jansen-Dürr, Premature senescence of human endothelial cells induced by inhibition of glutaminase, *Biogerontology* 9 (2008) 247–259, <https://doi.org/10.1007/s10522-008-9134-x>.
- [49] R. Cipriano, C.E. Kan, J. Graham, D. Danielpour, M. Stampfer, M.W. Jackson, TGF- β signaling engages an ATM-CHK2-p53-independent RAS-induced senescence and prevents malignant transformation in human mammary epithelial cells, *Proc. Natl. Acad. Sci. USA* 108 (2011) 8668–8673, <https://doi.org/10.1073/pnas.1015022108>.
- [50] Y. Guo, Y. Deng, X.Q. Li, Y. Ning, X.P. Lin, S.M. Guo, M.X. Chen, M. Han, Glutaminolysis was induced by TGF- β 1 through PP2Ac regulated Raf-MEK-ERK signaling in endothelial cells, *PLoS ONE* 11 (2016), e0162658, <https://doi.org/10.1371/journal.pone.0162658>.